

AD-A174 792

ELECTROMAGNETIC SENSOR ARRAYS FOR NONDESTRUCTIVE  
EVALUATION AND ROBOT CONTROL(U) SRI INTERNATIONAL MENLO  
PARK CA A J BAHR ET AL 30 OCT 86 AFOSR-TR-86-2025

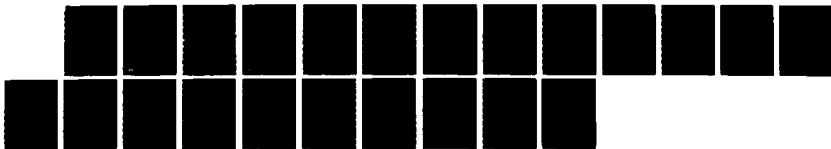
1/1

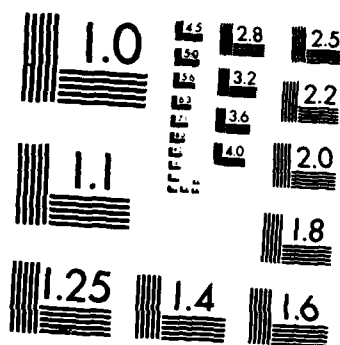
UNCLASSIFIED

F49620-84-K-0011

F/G 17/6

NL





MICROCOPY RESOLUTION TEST CHART  
NATIONAL BUREAU OF STANDARDS-1963-A

AD-A174 792

AFOSR-TR- 86-2025

(2)

# ELECTROMAGNETIC SENSOR ARRAYS FOR NONDESTRUCTIVE EVALUATION AND ROBOT CONTROL

By: A. J. BAHR A. ROSENGREEN

October 1986

Annual Technical Report

Covering the period 1 September 1985 - 31 August 1986

Prepared for:

AIR FORCE OFFICE OF SCIENTIFIC RESEARCH  
DIRECTORATE OF ELECTRONIC AND SOLID STATE SCIENCES  
BOLLING AIR FORCE BASE, BUILDING 410  
WASHINGTON, D.C. 20332

Attention: MAJOR J. W. HAGER  
Program Manager, AFOSR/Electronic & Materials Sciences

CONTRACT F49620-84-K-0011

SRI Project 7711

Approved for public release;  
distribution unlimited.

Approved for public release; distribution unlimited.

AIR FORCE OFFICE OF SCIENTIFIC RESEARCH (AFOSR)  
DIRECTORATE OF ELECTRONIC AND SOLID STATE SCIENCES

This technical report has been reviewed and is  
approved for public release to IAW AFR 190-12.  
Distribution unlimited.

MATTHEW J. KERRER  
Chief, Technical Information Division

DTIC FILE COPY

SRI International  
333 Ravenswood Avenue  
Menlo Park, California 94025  
(415) 326-6200  
Cable: SRI INTL MPK  
TWX: 910-373-2046

DTIC  
EXECTE  
DEC 3 1986



86 12 04 027

UNCLASSIFIED

SECURITY CLASSIFICATION OF THIS PAGE

ADA 174792

## REPORT DOCUMENTATION PAGE

1a. REPORT SECURITY CLASSIFICATION UNCLASSIFIED			1b. RESTRICTIVE MARKINGS NONE		
2a. SECURITY CLASSIFICATION AUTHORITY			3. DISTRIBUTION/AVAILABILITY OF REPORT APPROVED FOR PUBLIC RELEASE; DISTRIBUTION UNLIMITED		
2b. DECLASSIFICATION/DOWNGRADING SCHEDULE					
4. PERFORMING ORGANIZATION REPORT NUMBER(S) ANNUAL REPORT No. 2			5. MONITORING ORGANIZATION REPORT NUMBER(S) AFOSR-TR- 86-2025		
6a. NAME OF PERFORMING ORGANIZATION SRI INTERNATIONAL	6b. OFFICE SYMBOL (if applicable)	7a. NAME OF MONITORING ORGANIZATION Scum co 89			
6c. ADDRESS (City, State, and ZIP Code) 333 Ravenswood Avenue Menlo Park, California 94025		7b. ADDRESS (City, State, and ZIP Code) Scum co 8c			
8a. NAME OF FUNDING/SPONSORING ORGANIZATION USAF, AFSC	8b. OFFICE SYMBOL (if applicable) AFOSR/NE	9. PROCUREMENT INSTRUMENT IDENTIFICATION NUMBER CONTRACT No. F49620-84-K-0011			
8c. ADDRESS (City, State, and ZIP Code) Building 410 Bolling AFB, DC 20332		10. SOURCE OF FUNDING NUMBERS			
		PROGRAM ELEMENT NO. 6/6 2306	PROJECT NO. 2306	TASK NO. A2	WORK UNIT ACCESSION NO.
11. TITLE (Include Security Classification) Electromagnetic Sensor Arrays for Nondestructive Evaluation & Robot Control					
12. PERSONAL AUTHOR(S) A. J. Bahr and A. Rosengreen					
13a. TYPE OF REPORT ANNUAL	13b. TIME COVERED FROM 850901 TO 860831	14. DATE OF REPORT (Year, Month, Day) 1986 September 30		15. PAGE COUNT 17	
16. SUPPLEMENTARY NOTATION					
17. COSATI CODES			18. SUBJECT TERMS (Continue on reverse if necessary and identify by block number)		
FIELD 09	GROUP F	SUB-GROUP	Sensor, arrays, nondestructive evaluation, robotics, electromagnetic, imaging		
19. ABSTRACT (Continue on reverse if necessary and identify by block number) The objective of this research program is to develop the theoretical models, design methodology, and technology needed for optimum application of near-field electromagnetic sensor arrays in nondestructive evaluation (NDE) and robot control. This program is a collaborative effort by SRI and Stanford University. This report summarizes SRI's contribution to the program's second year research activities. SRI has demonstrated that small single-turn printed loops can be used as sensors with sufficient sensitivity to be useful in NDE and robotics and that printed-circuit techniques facilitate the fabrication of arrays of small loops to provide electronic scanning with high spatial resolution. SRI also has shown that deconvolution techniques can be used to improve the spatial resolution of such sensors in detecting edges and slots.					
20. DISTRIBUTION/AVAILABILITY OF ABSTRACT <input type="checkbox"/> UNCLASSIFIED/UNLIMITED <input checked="" type="checkbox"/> SAME AS RPT. <input type="checkbox"/> DTIC USERS			21. ABSTRACT SECURITY CLASSIFICATION		
22a. NAME OF RESPONSIBLE INDIVIDUAL Dr. Witt			22b. TELEPHONE (Include Area Code) 767 4984		22c. OFFICE SYMBOL N6

DD FORM 1473, 84 MAR

83 APR edition may be used until exhausted.  
All other editions are obsolete.

SECURITY CLASSIFICATION OF THIS PAGE

UNCLASSIFIED

# SRI International



## **ELECTROMAGNETIC SENSOR ARRAYS FOR NONDESTRUCTIVE EVALUATION AND ROBOT CONTROL**

*By:* A. J. BAHR      A. ROSENGREEN

*October 1986*

*Annual Technical Report*

*Covering the period 1 September 1985 - 31 August 1986*

*Prepared for:*

AIR FORCE OFFICE OF SCIENTIFIC RESEARCH  
DIRECTORATE OF ELECTRONIC AND SOLID STATE SCIENCES  
BOLLING AIR FORCE BASE, BUILDING 410  
WASHINGTON, D.C. 20332

Attention: MAJOR J. W. HAGER  
Program Manager, AFOSR/Electronic & Materials Sciences

CONTRACT F49620-84-K-0011

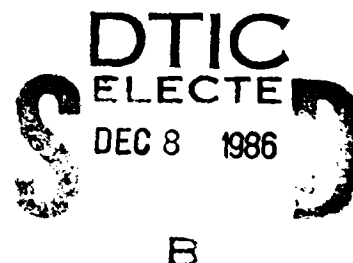
SRI Project 7711

Approved for public release; distribution unlimited.

*Approved by:*

TAYLOR W. WASHBURN, *Director*  
*Remote Measurements Laboratory*

LAWRENCE E. SWEENEY, JR., *Vice President*  
*System Technology Division*



SRI INTERNATIONAL, 333 Ravenswood Avenue, Menlo Park, California 94025  
(415) 326-6200, Cable: SRI INTL MPK, TWX: 910-373-2046

## CONTENTS

LIST OF ILLUSTRATIONS. . . . .	iv
I INTRODUCTION. . . . .	1
II RESEARCH STATUS . . . . .	3
A. Printed-Loop Sensor Arrays. . . . .	3
B. Imaging . . . . .	9
III SUMMARY . . . . .	14
APPENDIX A--INTERACTIONS AND PERSONNEL . . . . .	A-1
REFERENCES . . . . .	R-1



Accession	✓
NTIS	
DTIC	
Un	
PER CALL JC	
A	
DTIC	
A-1	

## ILLUSTRATIONS

Figure 1.	Vertical printed-loop sensor array. . . . .	4
2.	Horizontal printed-loop sensor array. . . . .	5
3.	Measurement setup . . . . .	6
4.	Spatial resolution of horizontal printed-loop sensor. . . .	6
5.	Step response of horizontal printed-loop sensor . . . . .	7
6.	Lift-off signal vs. distance (sum mode) . . . . .	8
7.	Measured line spread function of wire-coil sensor . . . . .	10
8.	Measured wide-slot response of wire-coil sensor . . . . .	11
9.	Effect of threshold level on deconvolution. . . . .	12

## I INTRODUCTION

The objective of this research program is to develop the theoretical models, design methodology, and technology needed for the optimum application of near-field electromagnetic sensor arrays in nondestructive evaluation (NDE) and robot control. This program is a collaborative effort by SRI and Stanford University, supported by separate contracts. This report summarizes SRI's contribution to this research during the program's second year.

The electromagnetic sensors being considered here fall into two main classes: inductive (magnetic) and capacitive (electric). During the past year, the work at SRI focused on the development of arrays of small inductive sensors, and the work at Stanford University emphasized the use of capacitive sensors. While inductive sensors have been used in NDE for many years, the technology traditionally used for fabricating such sensors is not well suited for constructing arrays. Since arrays are the main topic of this research, much of the effort at SRI during the past year has been devoted to developing and evaluating a suitable array-fabrication technology.

A literature search for fabrication technologies was begun last year and continued during the first part of this year. This search identified three potentially useful technologies: (1) magnetic thin-film technology used for read-write heads, (2) magneto-resistive thin-film technology used for read-only heads, and (3) metallic printed-circuit technology used for electronic integrated circuits. As discussed in last year's annual report,<sup>1</sup> magnetic thin-film technology was ruled out for our application because sensors that were made using this technology appeared to require very small lift-off distances for successful operation. Magneto-resistive technology appeared more promising, but it is not readily available to SRI. Hence, based on some promising results, reported in the literature,<sup>2</sup> that used small loops etched in a thin-film conductor to map magnetic fields near a recording head, and because printed-circuit technology is similar and readily available, we decided to evaluate experimentally a sensor array composed of printed loops. The results of that evaluation are very encouraging and are reported here.



Work also was begun last year to study the use of deconvolution algorithms for improving the spatial resolution of sensor arrays. A limited amount of work done during this year on this topic used experimental data to demonstrate the promise of this technique. The results of this demonstration also are included in this report.

## II RESEARCH STATUS

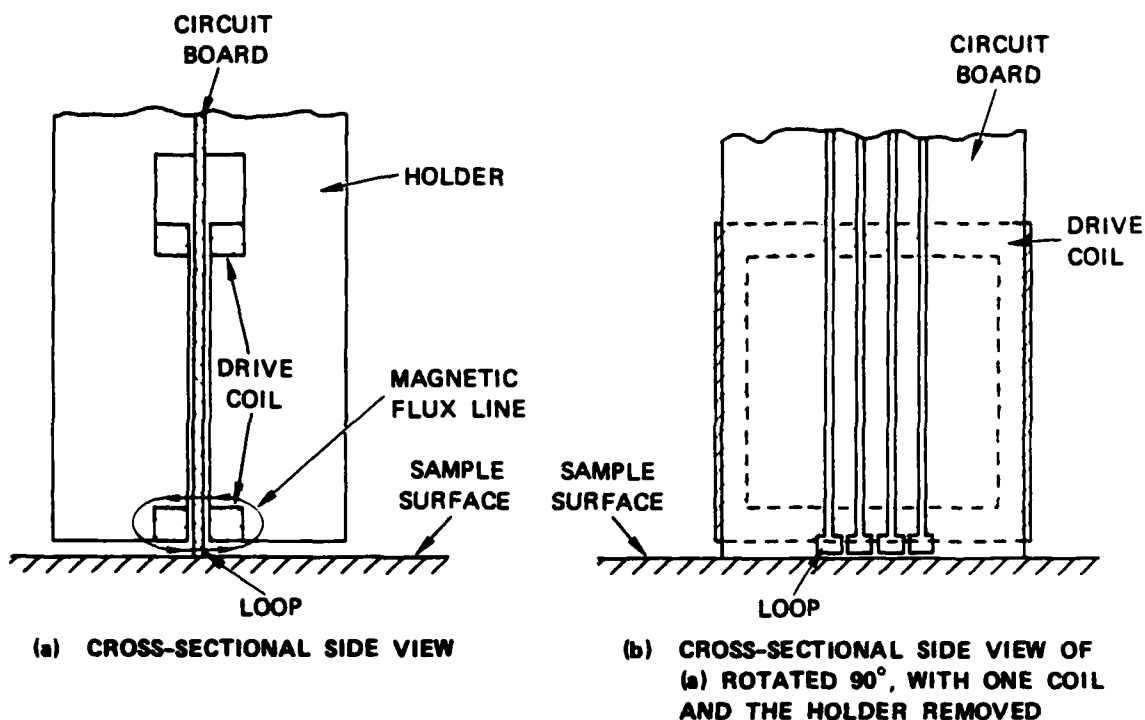
### A. Printed-Loop Sensor Arrays

The wire-wound coil sensor, which consists of a drive coil and several smaller pickup coils and which was discussed in last year's annual report,<sup>1</sup> uses a technology that is not well suited for constructing an array. Furthermore, the spatial resolution of such a sensor is limited by the minimum practical size of the pickup coils. To overcome these limitations, SRI built and evaluated a sensor using printed-circuit technology, which is expected to simplify the fabrication of an array, permit precise replication of the array elements, reduce the minimum achievable size of individual array elements to improve spatial resolution, and allow the construction of two-dimensional arrays.

Printed-circuit technology is widely used for fabricating planar circuit patterns and can produce line widths and spacings as small as a few thousandths of an inch. The use of this technology for inductive sensor arrays requires that the multi-turn coils used previously be replaced with single-turn printed loops. Although small single-turn loops reduce the sensor signal, they significantly improve spatial resolution.

A potentially useful feature of printed-circuit technology is that the circuit boards can be mounted in a vertical position with respect to the test sample to facilitate external connection to the sensor array (Figure 1). The cross-sectional side view in Figure 1(a) shows two vertical wire-wound drive coils and a circuit board containing the printed loops sandwiched between the coils. The relative position of the loops is shown in Figure 1(b).

The principle of operation of the printed-loop sensor is the same as that of an eddy-current reflection probe; that is, the sensor output is proportional to any change that occurs in the mutual coupling between the drive coil and pickup loops. The single magnetic flux line in Figure 1(a) schematically represents this mutual coupling.



TMS-2576

Figure 1. Vertical printed-loop sensor array.

First, a vertical sensor array was built and tested with two of the loops differentially connected. However, even when the sensor was scanned over the edge of a flat metal sample, the signal produced was very weak and could be only marginally detected because the magnetic fields responsible for the mutual coupling between the drive coils and the printed loops were not tightly coupled to the sample.

To improve the sensitivity of the sensor the vertical sensor array was converted to a horizontal sensor array with a single drive coil (Figure 2). As shown in Figure 2(a), the single drive coil with 5 x 6 turns and the circuit board are located parallel to the sample surface. The circuit board is between the drive coil and the test sample at a position close to the center of the drive coil. The array of the four printed loops, two of which are shown in Figure 2(b), fits well within the 0.5-in. x 0.5-in. opening of the drive coil. Each loop, formed by a 0.005-in.-wide printed conductor, has inside dimensions of 0.03 in. x 0.05 in. The center-to-center spacing between neighboring loops is 0.07 in. To reduce the electromagnetic pickup in the lines that connect the loops to the soldering pads, the entire board is wrapped with a 0.004-in.-thick copper foil so that only the loops are directly exposed to the magnetic field of the drive coil. A 0.002-in.-thick film of Kapton provides insulation between the loops and the copper foil. The copper foil typically touches the sample surface as shown, thus resulting in a lift-off distance of 0.006 in.

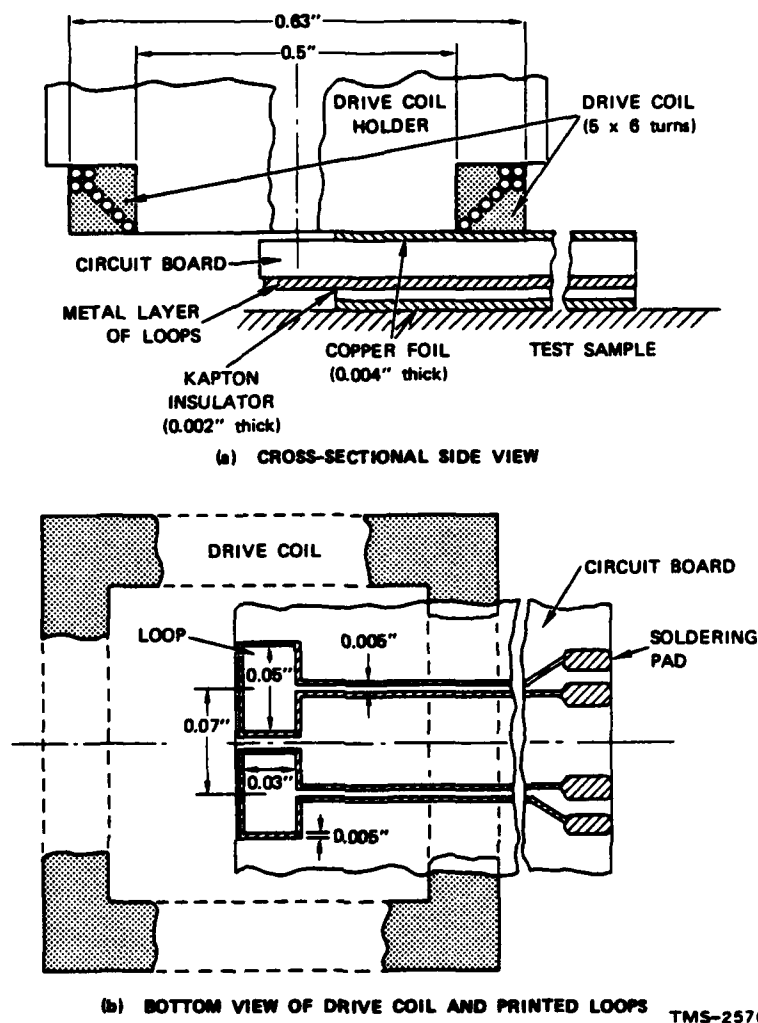


Figure 2. Horizontal printed-loop sensor array. (Not to scale.)

In the spatial-resolution and sensitivity experiments discussed below, the sensing loops were connected differentially as indicated in Figure 3, which also shows the measurement setup. The drive coil is excited by a stable 200-kHz signal, with a level such that the current in the coil is a few mA. The signals from the loops are sent to a differential amplifier via two potentiometers that are used to balance the sensor pair. The differential signal is detected by a lock-in amplifier that provides a full-scale 10-V output. This output is captured by the data acquisition system described in last year's annual report.<sup>1</sup> Although a

lock-in amplifier in the detection system is not essential, it was used for these experiments because of initial uncertainty about the sensitivity of the single-loop sensors.

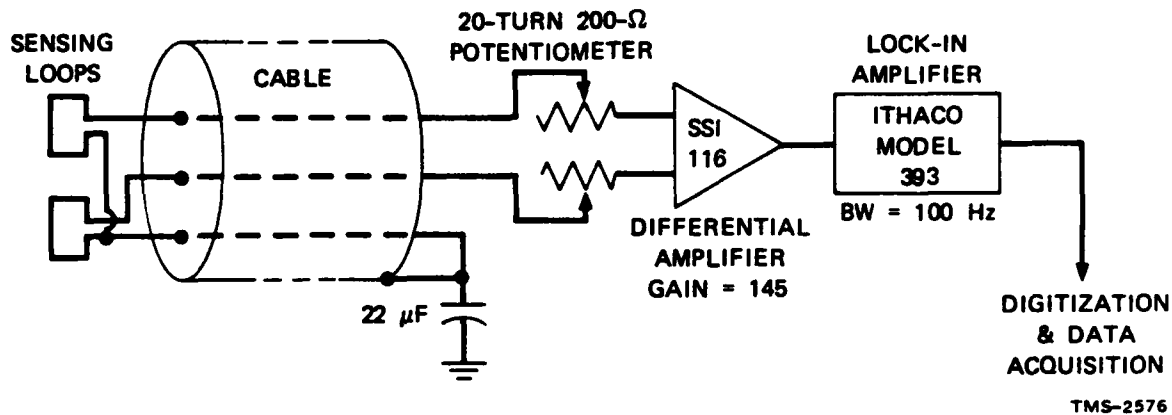


Figure 3. Measurement setup.

Figure 4 shows the improved spatial resolution of the printed-loop sensor over the wire-coil sensor described in last year's report.<sup>1</sup> Figure 4(a) compares the signals detected by a printed-loop and a wire-coil sensor when scanned over a wide

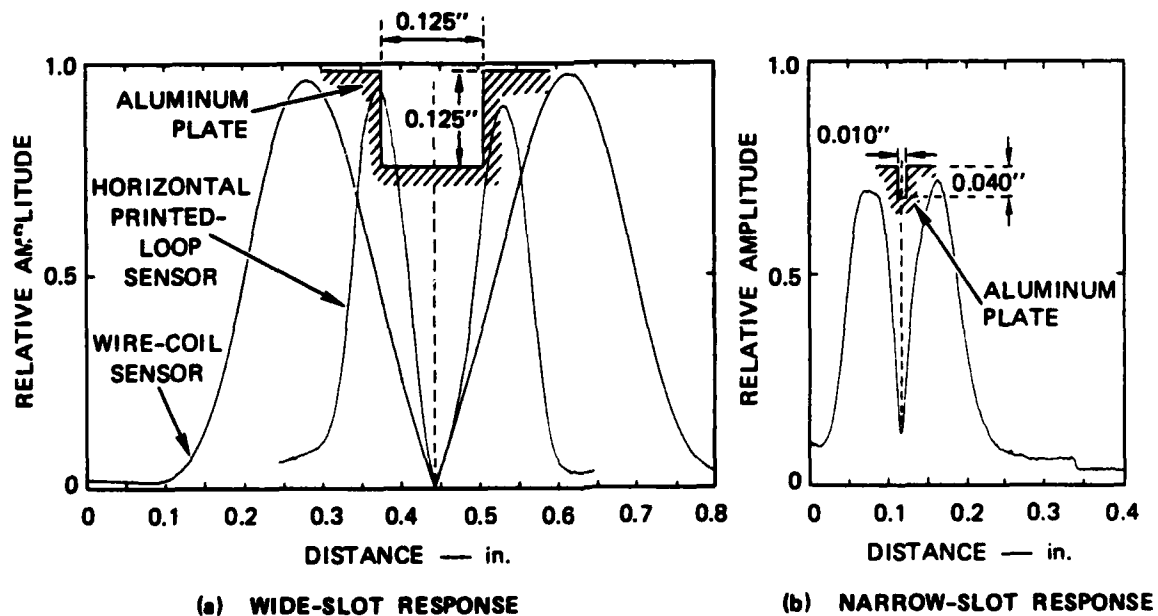
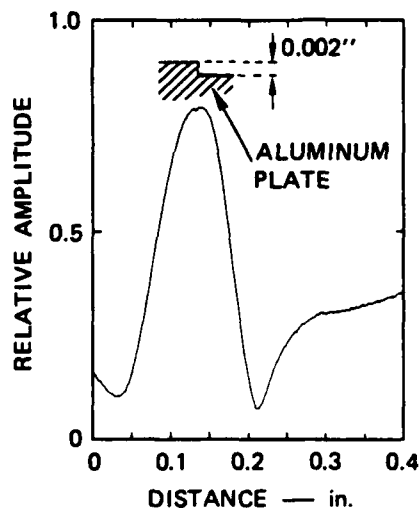


Figure 4. Spatial resolution of horizontal printed-loop sensor.

slot (0.125-in. wide and 0.125-in. deep) in an aluminum plate. Because it has a center-to-center spacing of 0.070 in., the printed-loop sensor is able to resolve the slot, whereas the wire-coil sensor, which has a center-to-center spacing four times larger, exhibits a response that is determined by the dimensions of the sensor and not those of the slot. Figure 4(b) shows the signal detected by a printed-loop sensor when scanned over a narrow EDM slot (0.010-in. wide and 0.040-in. deep) in an aluminum plate. As expected, the basic resolution of the differentially connected printed-loop sensor is about 0.070 in.

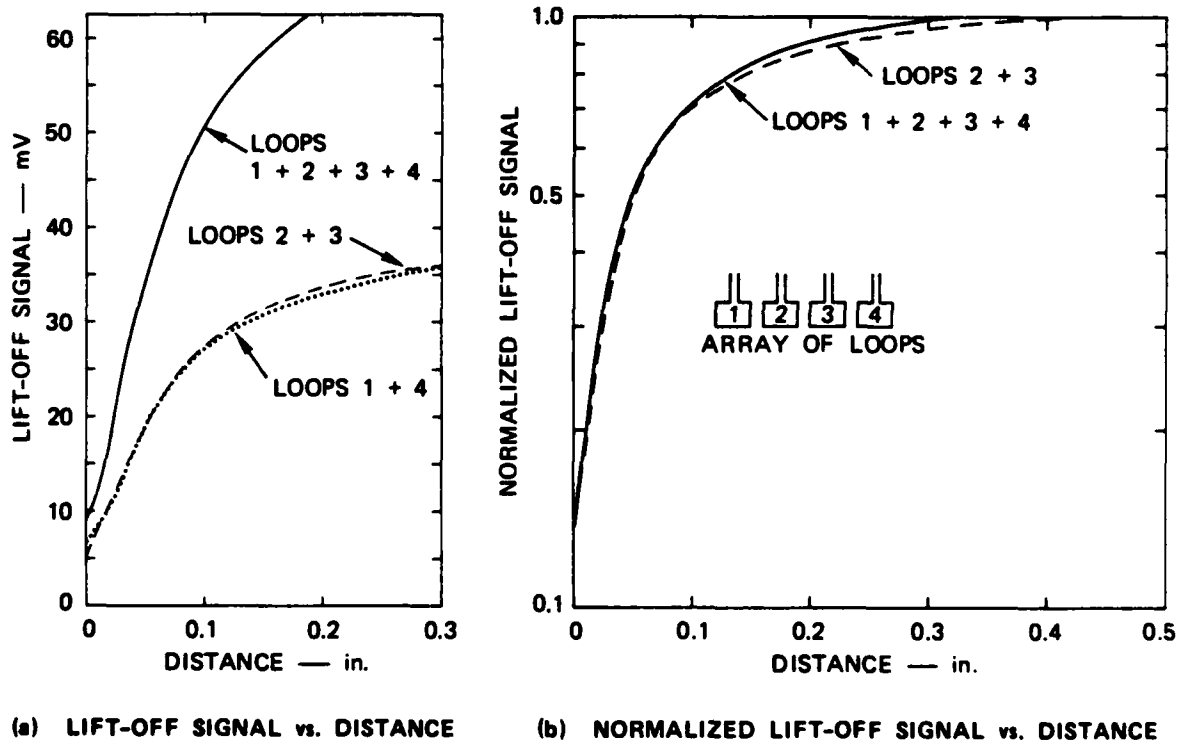
We evaluated the sensitivity of the horizontal printed-loop sensor by scanning small steps in an aluminum plate. Figure 5 shows the response to a 0.002-in. step. The full scale of this figure corresponds to a 30- $\mu$ V output from the differential amplifier. The voltage signal-to-noise ratio is larger than 100. This ratio is determined not only by the bandwidth, but also by the common-mode rejection of the differential amplifier. The common-mode rejection governs how large a signal can be applied to the drive coil before the common mode begins to mask a weak signal. In this case, the common-mode rejection was measured to be 60 dB. The drive current used to obtain the results shown in Figure 5 was 3-4 mA. For the signal level present in Figure 5, there was some common-mode interference, so the exact shape of the skirts of the curve depended on how the probe was aligned.



TMS-2576

Figure 5. Step response of horizontal printed-loop sensor.

When the loops are connected so that the signals from each loop add together rather than subtract, the sensor becomes very sensitive to lift-off. Using this sum mode, the probe becomes a proximity sensor. Figure 6 shows the results of varying the lift-off distance. In Figure 6(a), curves of the lift-off signal at the output of the preamp are drawn as functions of lift-off distance for the two cases where either two or four loops are connected in series. As can be seen, increasing the number of connected loops increases the sensitivity. Connecting either loops 2 and 3 or 1 and 4 made no difference in the detected signal. The output voltage appears to be simply the sum of the voltage from each loop, and there is no evidence of interaction between the loops. At 0.4 in. to 0.5 in. away from the sample, the lift-off voltage saturates. Using this saturation voltage to normalize the curves in Figure 6(a) produces the curves shown in Figure 6(b). These curves show that the range of lift-off distance over which the test piece exerts an influence on the detected signal is about 0.1 in. for both combinations of loops. Controlling this range of influence will probably require changing both the drive-field configuration and the loop interconnections. At present only one drive coil is used, but it may be possible to use an array of several localized drive coils to control the ranging effect.



TMS-2576

Figure 6. Lift-off signal vs. distance (sum mode).

## B. Imaging

Electromagnetic sensor arrays potentially may be used to "image" material or geometrical discontinuities in a workpiece being inspected. If the array elements are small enough compared to the size of the discontinuity, a reasonably precise two-dimensional picture can be formed that shows the extent and shape of the discontinuity. Such imaging is made possible by the fact that the electromagnetic fields involved in the interaction between the sensor and the discontinuity are quasi-static and, therefore, highly localized.

In general, however, the minimum size of an array element is limited by fabrication technology and there is usually a desire to improve upon the basic resolution that the sensor element provides. Such image enhancement can often be obtained by appropriately processing the measured data.

The output produced by an inductive sensor when it is scanned over an arbitrary discontinuity often can be represented as the convolution of the desired quasi-static image with the response of the sensor to a point imperfection.<sup>1,3,4</sup> This latter response is called the point spread function of the sensor. Hence, image enhancement can be obtained in this case by deconvolving the measured sensor response with its point spread function.

There are a number of algorithms for deconvolving two functions. The simplest one to understand is based on the fact that the Fourier transform of a convolution is the product of the Fourier transforms of the two functions being convolved, that is,

$$V(k) = PS(k) \cdot IM(k) \quad , \quad (1)$$

where  $k$  represents spatial frequency,  $V(k)$  is the transformed measured sensor voltage,  $PS(k)$  is the transformed point spread function, and  $IM(k)$  is the transformed image. Hence, the desired image is given by the inverse Fourier transform of the ratio:

$$IM(k) = \frac{V(k)}{PS(k)} \quad . \quad (2)$$

The point spread function,  $PS(k)$ , represents a spatial filter that operates on the quasi-static image fields to produce the measured voltage. This filter must have adequate spatial bandwidth if a good image is to be obtained by

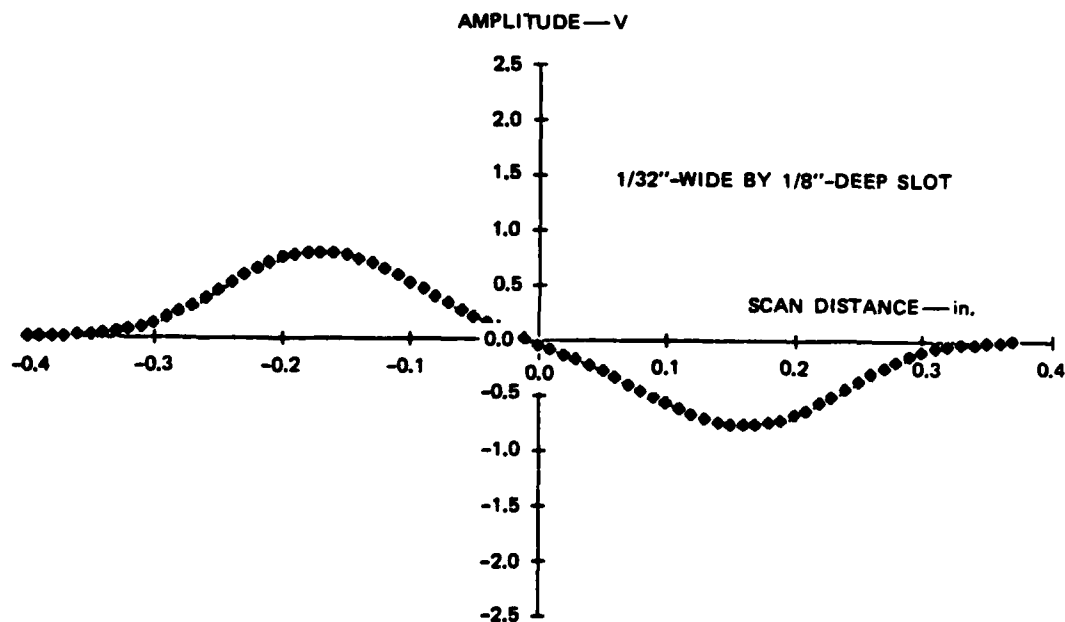


deconvolution. Also, numerical difficulties arise at spatial frequencies where  $PS(k)$  is small because of the inevitable presence of noise. The results to be presented here were obtained by applying the regularizing algorithm:

$$IM(k) = 0, \text{ if } PS(k) \text{ is less than or equal to } T, \quad (3)$$

where  $T$  is an empirical threshold level.

Data were taken by scanning long slots in flat aluminum plates using the wire-coil sensor described in last year's report.<sup>1</sup> Since the dimensions of this sensor are relatively large, its point spread function (or, as in this case for a long slot, its line spread function) was obtained to good accuracy by measuring a slot 1/32-in. wide by 1/8-in. deep. The data that define this function are shown plotted versus scan distance in Figure 7. The spatial extent of this function is about 0.5 in., which is determined by the dimensions and spacing of the sense coils. The Fourier transform of this function has its major peak at about 1.4 in.<sup>-1</sup>, but contains significant spectral energy out to spatial frequencies of about twice this value. Thus, one expects that the deconvolution of slot data obtained using this sensor will produce significant image improvement for slots with widths as narrow as 0.25 in.



TMS-2576

Figure 7. Measured line spread function of wire-coil sensor.

A 0.25-in.-wide by 0.125-in.-deep slot was measured to test this assertion, and the data are shown in Figure 8. To illustrate the effect that the choice of threshold value,  $T$ , in the regularizing algorithm has on the deconvolution results, Figures 9(a), (b), and (c) show the results for three values of  $T$ . The unprocessed measured data are shown in all three figures for comparison. The objective of processing these data is to obtain a sensor signal whose peaks occur at the edges of the slot so that the slot width can be estimated accurately.

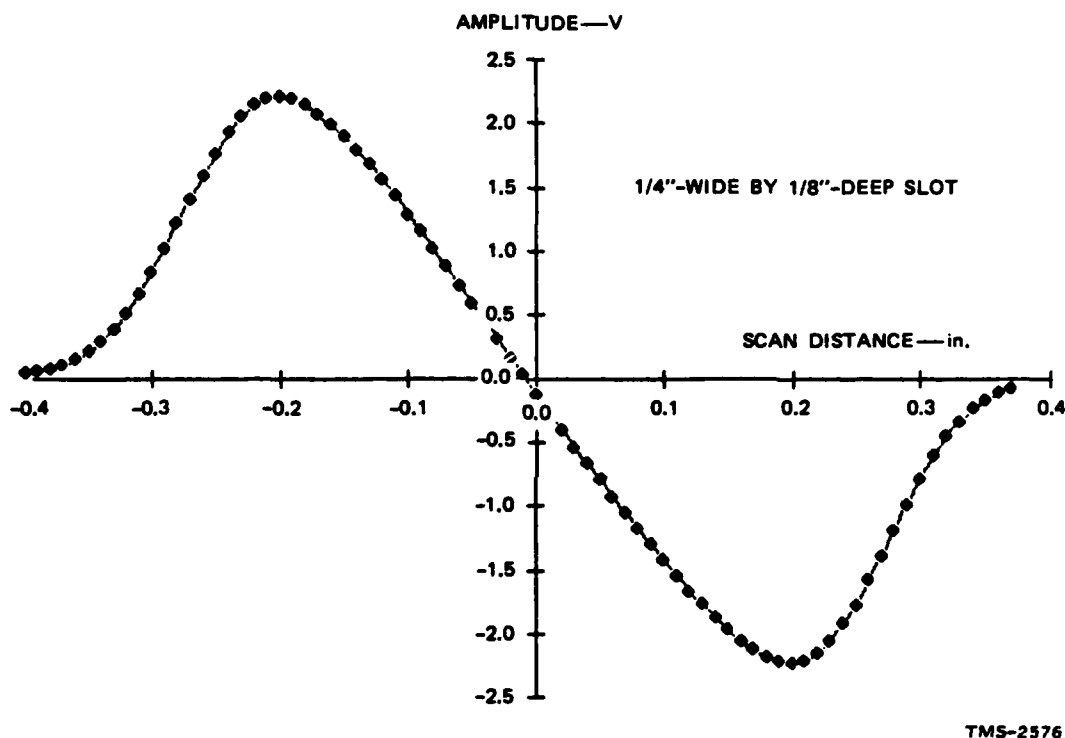


Figure 8. Measured wide-slot response of wire-coil sensor.

Figure 9(a) shows the effect of making the threshold too high. In this case, the regularization suppresses the higher spatial frequencies, and it is not possible to move the positions of the peaks in the detected signal very much. Figure 9(b) shows the results obtained using the optimum threshold value. In this case the signal peaks are aligned very closely with the slot edges, thus proving the assertion that image enhancement is possible for this slot width. The distance between the peaks of the processed signal predicts the correct slot width to within  $\pm 0.02$  in., whereas the slot width predicted by the unprocessed data is in error by

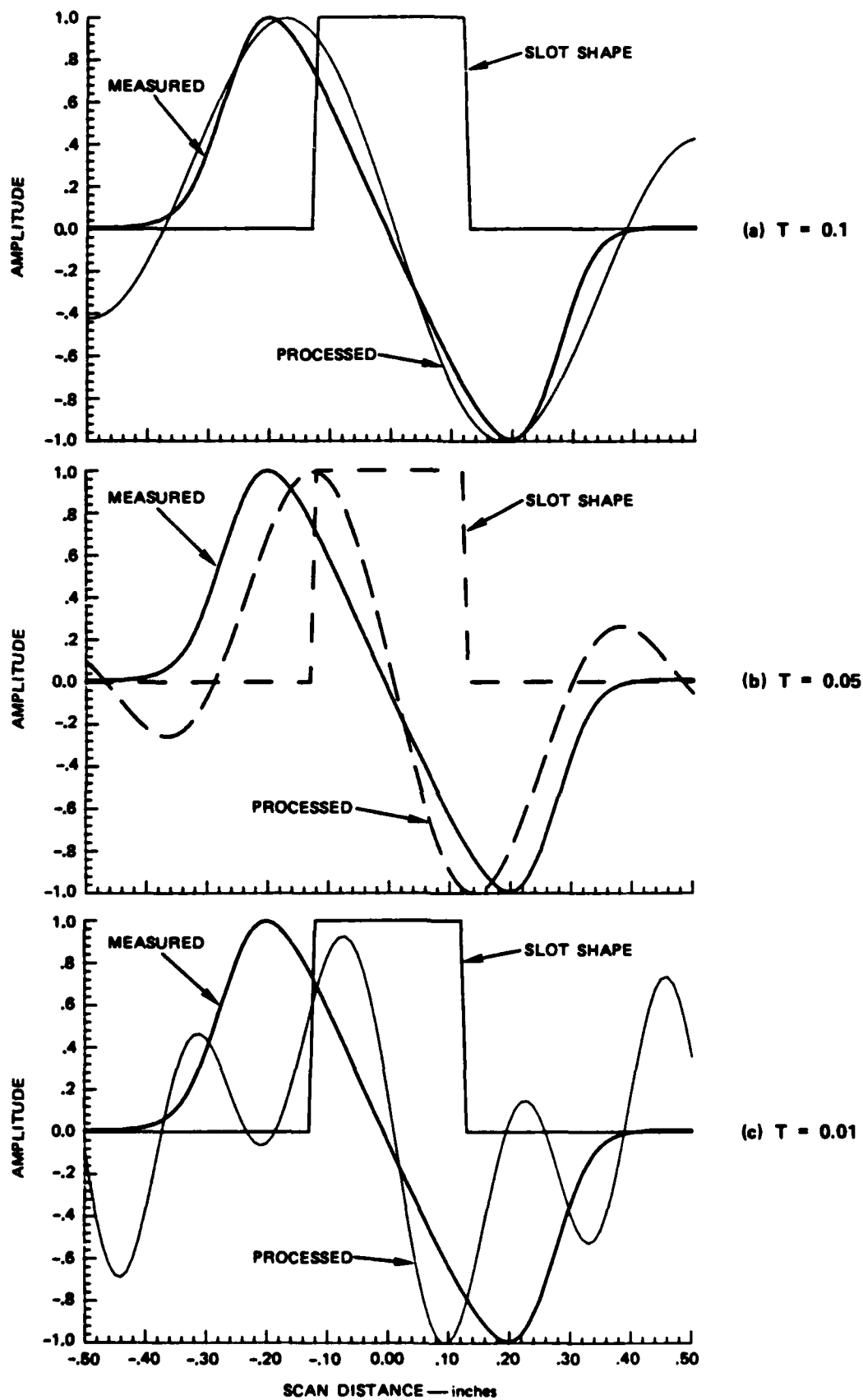


Figure 9. Effect of threshold level on deconvolution.

0.16 in. Finally, Figure 9(c) shows the effect of using too small a threshold value. In this case, spurious spatial frequencies are introduced and one loses the ability to interpret the sensor signal properly.

From these results SRI concludes that further study of deconvolution techniques is worthwhile for the purpose of improving the spatial resolution of electromagnetic sensor arrays beyond that provided by reducing the size of the array elements.

#### IV SUMMARY

It has been demonstrated that small single-turn printed loops can be used as sensors with sufficient sensitivity to be useful in NDE and robotics and that printed-circuit techniques facilitate the fabrication of arrays of small loops to provide electronic scanning with high spatial resolution. It has also been shown that deconvolution techniques improve the spatial resolution of such sensors in detecting edges and slots. Future research plans under this contract include developing a model for inductive sensor arrays; designing and building a horizontal-loop array with vertical connections; demonstrating electronic scanning in one, and perhaps two, dimensions; and exploring the possibilities of arraying drivers as well as sensors.

## APPENDIX A

### A. Interactions

1. B. A. Auld and A. J. Bahr, "A Novel Multifunction Robot Sensor," presented at the 1986 IEEE International Conference on Robotics and Automation, San Francisco, California, April 1986, and published in the conference proceedings.
2. A. Rosengreen and A. J. Bahr, "Inductive Sensor Arrays for NDE and Robotics," presented at the Review of Progress in Quantitative NDE, La Jolla, California, August 1986. To be published in the conference proceedings.

### B. Personnel

Dr. A. J. Bahr, Staff Scientist and Principal Investigator  
Mr. D. W. Cooley, Sr. Research Engineer  
Mr. M. R. Cutter, Engineering Assistant  
Mr. W. B. Weir, Sr. Research Engineer

### C. Acknowledgment

As extremely important element in this program is the close collaboration that exists between SRI personnel and Professor B. A. Auld and his students at Stanford University.

## REFERENCES

1. A. J. Bahr and A. Rosengreen, "Electromagnetic Sensor Arrays for Nondestructive Evaluation and Robot Control," Annual Technical Report on Contract F49620-84-K-0011, SRI Project 7711, SRI International, Menlo Park, California, (October 1985).
2. R. F. Hoyt, et al., "Direct Measurement of Recording Head Fields Using a High-Resolution Inductive Loop," Journal of Applied Physics, Vol. 55, pp. 2241-2244, (March 15, 1984)
3. B. A. Auld, J. Kenney, and T. Lookabaugh, "Electromagnetic Sensor Arrays--Theoretical Studies," Review of Progress in Quantitative Nondestructive Evaluation, Vol. 5, D. O. Thompson and D. E. Chimenti, Editors, pp. 681-690, (Plenum Press, New York, 1985).
4. R. O. McCary, D. W. Oliver, K. H. Silverstein, and J. D. Young, "Eddy Current Imaging," IEEE Transactions on Magnetics, Vol. MAG-20, pp. 1986-1988 (September 1984).

END

1-87

DT/C